SUPPLMENTARY MATERIAL

GC-MS profiling of *Vitex pinnata* bark lipophilic extract and screening of its anti-TB and cytotoxic activities.

Safa Abdelbaset [a], Dina M. El-Kersh[a,b], Iriny M. Ayoub[c], Omayma A. Eldahshan[c,d *]

[a] Pharmacognosy Department, Faculty of Pharmacy, The British University in Egypt (BUE), Cairo 11837, Egypt; safa.abdelbaset@bue.edu.eg and dina.elkersh@bue.edu.eg orcid.org/0000-0002-4782-8396

[b] Center for Drug Research and Development (CDRD), The British University in Egypt (BUE), Cairo 11837, Egypt

[c] Pharmacognosy Department, Faculty of Pharmacy, Ain Shams University, Cairo Governorate 11566, Egypt; irinyayoub@pharma.asu.edu.eg orcid.org/0000-0003-2382-8241 and oeldahshan@pharma.asu.edu.eg orcid.org/0000-0002-0972-0560

[d] Center for Drug Discovery Research and Development, Ain Shams University, Egypt

[*]Correspondence:
Omayma A. Eldahshan: e-mail address: oeldahshan@pharma.asu.edu.eg

ABSTRACT

Tuberculosis is a highly infectious ailment worldwide. The emergence of multi-drug resistance and serious adverse effects of anti-TB drugs have led to the continuous search of natural candidates. This study aimed to analyze the chemical profile of *Vitex pinnata* (VP) bark lipophilic extract using GC-MS for the first time also evaluating its anti-TB and cytotoxic activities. GC-MS revealed a total of 81 compounds which representing 86% identified compounds. *In vitro* anti-TB of VP lipophilic extract was evaluated using the Microplate Alamar Blue Assay which exhibited MIC value of 62.5 µg/mL. *In vitro* cytotoxicity was evaluated using Water Soluble formazan assay recording IC_{50} > 100 and 200 µg/mL using Vero and A-549 cell lines; respectively. *In silico* docking study was performed on the major identified compounds, *n*-nonane showed the most favorable binding affinity (ΔG) equals to -33.34 Kcal/mol. The results obtained herein unraveled the potential use of VP *n*- hexane extract as a natural anti-TB.

KEYWORDS: *Vitex pinnata* bark; GC-MS; anti-TB; Microplate Alamar Blue Assay; Cell viability; WST-1; Molecular docking

Experimental section

Plant material and solvents

V. pinnata bark was collected in November 2019 from a local plantation located in Gerik, Perak, Malaysia. The plant was purchased and authenticated from ETHNO Resources Sdn. Bhd. (846944-K) herbal company, Selangor Malaysia (http://ethnoherbs.net/). A voucher specimen (PHG-P-VP-302) was deposited in the herbarium of Pharmacognosy Department, Faculty of Pharmacy, Ain Shams University, Cairo, Egypt. *n*-Hexane was purchased from Tedia® (Ohio, USA).

Comment [sa1]: Collection date

Preparation of the plant extract

Four kilograms of *V. pinnata* bark powder were defatted by *n*-hexane at room temperature then concentrated *in vacuo* using rotary evaporator (Büchi Labortechnik GmbH, Essen, Germany). A yellowish extract (18.7 g) (0.46% w/w) was then obtained and kept at -8°C till further analysis.

GC-MS analysis procedure

Diluted sample (1% *v/v*) of *n*-hexane extract of *V. pinnata* bark with *n*-hexane solvent was analyzed using GC-MS (Shimadzu-QP2010, Koyoto, Japan) equipped with RTX-5MS fused bonded column (30 m x 0.25 mm i.d., x 0.25 µm film thickness) (Restek, USA). The initial column temperature was maintained at 45°C for 2 min (isothermal), then programmed to 300°C at a rate of 5°C/min and kept constant at 300°C for 5 min (isothermal). Injector temperature was 250°C. The flow rate of helium as a carrier gas was 1.41 mL/min. All the mass spectra were recorded under the following conditions: (equipment current) filament emission current, 60 mA; ionization voltage, 70 eV; ion source, 200°C. The sample was injected at a split ratio 1: 15. Retention indices (RI) were calculated relative to standard *n*-alkanes series (C_8-C_{40}) injected under similar conditions. Identification of compounds was performed by comparing the mass spectra and retention indices with those of the National Institute of Standards and Technology NIST chemistry webbook library and literature (Abd El-Ghffar et al. 2017, Abd El-Ghffar et al. 2018, Adams 2007, Al-Sayed et al. 2021, Ashmawy et al. 2021, Ayoub et al. 2021, Gad et al. 2021, Korany et al. 2021, Thabet et al. 2021).

Microplate Alamar Blue Assay (MABA)

MABA is an *in vitro* screening assay that allows for the quantitative determination of drug susceptibility against any strain of replicating *Mycobacterium tuberculosis* (Nkenfou et al. 2015). Antimycobacterial activity was evaluated against *Mtb* (ATCC 27294) strain obtained from the culture collection of the Regional Center for Mycology and Biotechnology (RCMB), Al-Azhar University (Cairo, Egypt), in which the susceptibility test was designed as previously described by (Franzblau et al. 1998) with some modifications. Black, clear-bottomed, 96 well microplates, with outer perimeter wells filled with sterile water to prevent well dehydration. The initial dilutions of VP *n*-hexane extract were prepared in dimethyl sulfoxide (DMSO) followed by two-fold serial dilutions in the microplates. The test concentrations ranged between (125-0.24 µg/mL). *Mtb* inoculum was diluted and added with approximately 0.1 mL of (1x 10^5 CFU/mL) to the wells containing the VP *n*-hexane extract. Additional wells composed only from *Mtb* act as control. The microplates were incubated at 37°C for 4 days. After the incubation period, 20 µL of Alamar blue solution (Alamar Biosciences/Accumed, Westlake, OH, USA) and 12.5 µL of 20 % Tween 80 were added to the plates which were re-incubated at 37°C for 24 hours. The results were

measured and recorded at 590 nm. Isoniazid (Sigma Aldrich, St. Louis, US) was used as a positive control with concentrations varying from (31.25-0.06µg/mL). Visual minimal inhibitory concentration (MIC) was defined as the lowest concentration of the extract that prevents color changing from blue color which represents "no mycobacterial growth" to pink color ''growth occurrence". Also, it is defined as the lowest extract concentration inducing an inhibition of ≥90% of bacterial growth (Lawal et al. 2011). The MIC_{90} was evaluated as the concentration that prevents 90% of *Mtb* (Abdel-Aziz et al. 2020). The percent inhibition was calculated using the equation (Gamal El-Din et al. 2018):

$$\% \text{ Inhibition} = [1 - (\text{mean of test well/mean of bacterial wells})] \times 100$$

Cell lines and culture condition

Normal African Green Monkey Kidney (Vero) cells and non-small cell lung cancer (A-549) cells were obtained from Nawah Scientific Inc., (Mokatam, Cairo, Egypt). For routine maintenance, the cell lines were grown in Gibco Dulbecco's Modified Eagle Medium (DMEM) supplemented with 100 mg/mL of streptomycin, 100 units/mL of penicillin and 10% of heat-inactivated fetal bovine serum humidified in an atmosphere of 5% (*v/v*) CO_2 at 37°C.

In vitro cell viability and cytotoxicity using WST-1 assay

Cell viability assay is a colorimetric quantitative assay which measures the ability of cellular cleavage of the water-soluble tetrazolium salt using cellular mitochondrial dehydrogenase to dark yellow formazan dye (Kamiloglu et al. 2020). The number of viable cells is directly proportional to the amount of the dye produced using mitochondrial dehydrogenase. The cell viability was assessed by cell proliferation reagent WST-1 using Abcam® kit (ab155902 WST-1 Cell Proliferation Reagent). Vero and A-549 cells were seeded with 50 µL of culture medium ($3x10^3$ cells) using a 96-well plate. After 24-hour incubation, 50 µL culture media containing the VP *n*-hexane extract was added to cell lines at 10-fold serial dilution (100, 10, 1, 0.1, and 0.01 µg/mL) for Vero cells and (200, 20, 2, 0.2, and 0.02 µg/mL) for A-549 cells. After 48-hour incubation, 10 µL of WST-1 reagent was added to the treated cells. The absorbance was measured at 450 nm using a BMG LABTECH®- fluostar Omega microplate reader (Allmendgrün, Ortenberg, Germany). The results were performed in triplicates.

The inhibitory concentration of cell growth (IC_{50}) was assessed as the 50% reduction of U.V absorbance of treated cells *versus* control culture (Ahmad et al. 2010). The IC_{50} value was determined using Sigma Plot software, version 12.0 (System Software, San Jose, CA, USA).

The percentage of cell viability was calculated using the following equation (Kamiloglu et al. 2020).

$$\% \text{ Viability} = \frac{\text{Mean OD (sample)}}{\text{Mean OD (blank)}} \times 100$$

Whereas OD (sample)=Mean optical density of wells treated with the tested sample and OD (blank)=Mean optical density of untreated cells.

The relation between viable cells (%) and the extract concentrations (µg/mL) is plotted to get the survival curve on each cell lines after treatment.

In silico molecular docking study

The crystal structure of the molecular target *Mtb* C171Q receptor KasA inhibitor was retrieved from Protein Data Bank (http://www.rscb.org/pdb/) with PDB ID code (4C6X, 1.95 Å). The molecular docking was performed using Discovery Studio 4.5 software (Accelrys Inc., San Diego, CA, USA) by employing the C-docker algorithm as previously described (Ayoub et al. 2021, M Elkady et al. 2020). Validation of the docking procedure using C-docker protocol was achieved by calculating the root-mean-square deviations (RMSD) of thiolactomycin, the co-crystalized ligand that docked within the pocket of the active center and comparing it with the original co-crystallized inhibitor.

Tables (S1-S3)

Table S1. Chemical profiling of *n*-hexane extract of *V. pinnata* bark identified using GC-MS

Peak No.	Compound Name	Molecular Formula	Rt (min)	Area %	RI* Obs.	RI Lit.	Class	Identification
1	***n*-Nonane**	C_9H_{20}	6.075	**3.95**	900	900	Acyclic alkanes	MS, RI
2	2,6-Dimethyloctane	$C_{10}H_{22}$	7.055	1.65	934	935	Acyclic alkanes	MS, RI
3	2-Methyl nonane	$C_{10}H_{22}$	7.995	0.49	966	962	Acyclic alkanes	MS, RI
4	**2,3-Dimethyl-2-octene**	$C_{10}H_{20}$	8.3	**3.55**	976	977	Acyclic alkenes	MS, RI
5	**(*E*)-*p*-Menthane**	$C_{10}H_{20}$	8.572	**1.90**	985	984	Cyclic monoterpenes	MS, RI
6	***n*-Decane**	$C_{10}H_{22}$	9.157	**4.55**	1005	999	Acyclic alkanes	MS, RI
7	2,3-Dimethyl nonane	$C_{11}H_{24}$	9.745	1.69	1023	1024	Acyclic alkanes	MS, RI
8	Butyl cyclohexane	$C_{10}H_{20}$	10.121	1.48	1035	1031	Cyclic hydrocarbons	MS, RI
9	**(*E*)-Decahydronaphthalene**	$C_{10}H_{18}$	10.843	**2.57**	1058	1057	Aromatic hydrocarbons	MS, RI
10	5-Methyl decane	$C_{11}H_{24}$	10.945	0.65	1061	1058	Acyclic alkanes	MS, RI
11	4-Methyl decane	$C_{11}H_{24}$	11.045	0.63	1064	1059	Acyclic alkanes	MS, RI
12	2-Methyl decane	$C_{11}H_{24}$	11.160	1.53	1068	1061	Acyclic alkanes	MS, RI
13	3-Methyl decane	$C_{11}H_{24}$	11.365	1.64	1074	1069	Acyclic alkanes	MS, RI
14	***n*-Undecane**	$C_{11}H_{24}$	12.360	**14.51**	1106	1099	Acyclic alkanes	MS, RI
15	2-Methyldecahydronaphthalene	$C_{11}H_{20}$	12.618	0.77	1114	1115	Aromatic hydrocarbons	MS, RI
16	Pentyl cyclohexane	$C_{11}H_{22}$	13.38	1.22	1122	1130	Cyclic hydrocarbons	MS, RI
17	6-Methyl undecane	$C_{12}H_{26}$	14	1.39	1155	1155	Acyclic alkanes	MS, RI
18	4-Methyl undecane	$C_{12}H_{26}$	14.155	0.76	1164	1160	Acyclic alkanes	MS, RI
19	**2-Methyl undecane**	$C_{12}H_{26}$	14.297	**2.1**	1168	1167	Acyclic alkanes	MS, RI
20	3-Methyl undecane	$C_{12}H_{26}$	14.494	0.98	1174	1171	Acyclic alkanes	MS, RI
21	***n*-Dodecane**	$C_{12}H_{26}$	15.459	**9.93**	1206	1199	Acyclic alkanes	MS, RI
22	3,6-Dimethyl undecane	$C_{13}H_{28}$	15.818	1.1	1218	1210	Acyclic alkanes	MS, RI
23	6-Methyl dodecane	$C_{13}H_{28}$	16.951	0.2	1256	1253	Acyclic alkanes	MS, RI
24	2-Methyl dodecane	$C_{13}H_{28}$	17.278	0.23	1268	1268	Acyclic alkanes	MS, RI

25	4,6-Dimethyl dodecane	$C_{14}H_{30}$	17.534	0.17	1276	1285	Acyclic alkanes	MS, RI
26	*n*-Tridecane	$C_{13}H_{28}$	18.334	0.31	1304	1300	Acyclic alkanes	MS, RI
27	Phenyl cyclohexane	$C_{12}H_{16}$	18.98	0.02	1309	1308	Cyclic Hydrocarbons	MS, RI
28	2-Methyl tridecane	$C_{14}H_{30}$	20.11	0.11	1368	1365	Acyclic alkanes	MS, RI
29	2,6,10-Trimethyl dodecane	$C_{15}H_{32}$	20.464	0.12	1380	1379	Acyclic alkanes	MS, RI
30	*n*-Tetradecane	$C_{14}H_{30}$	21.116	1.11	1404	1399	Acyclic alkanes	MS, RI
31	2,6-Dimethyl naphthalene	$C_{12}H_{12}$	21.397	0.24	1415	1416	Aromatic hydrocarbons	MS, RI
32	1,3-Dimethyl naphthalene	$C_{12}H_{12}$	21.805	0.43	1430	1427	Aromatic hydrocarbons	MS, RI
33	2,6,10-Trimethyl tridecane	$C_{16}H_{34}$	22.748	0.48	1468	1465	Acyclic alkanes	MS, RI
34	*α*-Curcumene	$C_{15}H_{22}$	23.426	0.98	1492	1493	Sesquiterpenes	MS, RI
35	*β*-Eudesma-4(14),11-diene	$C_{15}H_{24}$	23.6	0.09	1478	1478	Sesquiterpenes	MS, RI
36	*n*-Pentadecane	$C_{15}H_{32}$	23.737	1.1	1504	1500	Acyclic alkanes	MS, RI
37	*α*-Muurolene	$C_{15}H_{24}$	23.93	0.2	1512	1511	Sesquiterpenes	MS, RI
38	*β*-Bisabolene	$C_{15}H_{24}$	24.087	0.09	1518	1518	Oxygenated sesquiterpenes	MS, RI
39	2,4-Di-tert-butylphenol	$C_{14}H_{22}O$	24.2	0.07	1523	1521	Alkyl phenol	MS, RI
40	*δ*-Cadinene	$C_{15}H_{24}$	24.512	0.16	1536	1536	Sesquiterpenes	MS, RI
41	2-Methyl pentadecane	$C_{16}H_{34}$	25.308	0.11	1568	1569	Acyclic alkanes	MS, RI
42	Nonane, 1-phenyl	$C_{15}H_{24}$	25.595	0.06	1579	1586	Alkylbenzene	MS, RI
43	Ar-Turmerol	$C_{15}H_{22}O$	25.91	0.15	1592	1594	Sesquiterpene alcohol	MS, RI
44	1-Hexadecene	$C_{16}H_{32}$	26.045	0.28	1597	1593	Acyclic alkenes	MS, RI
45	***n*-Hexadecane**	$C_{16}H_{34}$	26.214	**1.76**	1604	1600	Acyclic alkanes	MS, RI
46	Epicurzerenone	$C_{15}H_{18}O_2$	26.574	0.15	1620	1623	Oxygenated sesquiterpenes	MS, RI
47	*α*-Humulene epoxide II	$C_{15}H_{24}O$	26.72	0.07	1626	1620	Oxygenated sesquiterpenes	MS, RI
48	(1-Butylheptyl) benzene	$C_{17}H_{28}$	27.135	0.26	1644	1633	Alkylbenzene	MS, RI
49	2-Methyl hexadecane	$C_{17}H_{36}$	27.7	0.13	1668	1666	Alkylbenzene	MS, RI
50	Ar-Turmerone	$C_{15}H_{20}O$	27.97	0.37	1671	1670	Sesquiterpene alcohol	MS, RI
51	Norphytan	$C_{19}H_{40}$	28.688	0.51	1709	1707	Acyclic diterpenes	MS, RI
52	(1-Pentylheptyl) benzene	$C_{18}H_{30}$	29.312	0.13	1735	1727	Alkylbenzene	MS, RI
53	(1-Butyloctyl) benzene	$C_{18}H_{30}$	29.42	0.28	1740	1731	Alkylbenzene	MS, RI
54	(-)-Xanthorrhizol	$C_{15}H_{22}O$	29.951	0.32	1761	1758	Sesquiterpene alcohol	MS, RI
55	*α*-Octadecene	$C_{18}H_{36}$	30.648	0.11	1792	1792	Acyclic alkenes	MS, RI
56	*n*-Octadecane	$C_{18}H_{38}$	30.793	0.6	1796	1800	Acyclic alkanes	MS, RI
57	2-Methyloctadecane	$C_{19}H_{40}$	32.14	0.1	1865	1867	Acyclic alkanes	MS, RI

58	1-Nonadecene	$C_{19}H_{38}$	32.915	0.48	1905	1899	Acyclic alkenes	MS, RI
59	Palmitic acid, methyl ester	$C_{17}H_{34}O_2$	33.515	0.12	1935	1933	Fatty acid ester	MS, RI
60	*n*-Eicosane	$C_{20}H_{42}$	34.94	0.52	2005	2000	Acyclic alkanes	MS, RI
61	2-Methyl eicosane	$C_{21}H_{44}$	36.17	0.07	2069	2064	Acyclic alkanes	MS, RI
62	1-Octadecanol	$C_{18}H_{38}O$	36.327	0.13	2077	2077	Fatty alcohol	MS, RI
63	*n*-Heneicosane	$C_{21}H_{44}$	36.876	0.41	2106	2100	Acyclic alkanes	MS, RI
64	Phytol	$C_{20}H_{40}O$	37.22	0.31	2124	2122	Acyclic diterpene alcohol	MS, RI
65	*n*-Docosane	$C_{22}H_{46}$	38.733	0.54	2206	2200	Acyclic alkanes	MS, RI
66	*n*-Tricosane	$C_{23}H_{48}$	40.511	0.62	2307	2300	Acyclic alkanes	MS, RI
67	*n*-Tetracosane	$C_{24}H_{50}$	42.210	0.92	2406	2400	Acyclic alkanes	MS, RI
68	*n*-Pentacosane	$C_{25}H_{52}$	43.860	1.46	2508	2500	Acyclic alkanes	MS, RI
69	*n*-Hexacosane	$C_{26}H_{54}$	45.425	0.43	2608	2600	Acyclic alkanes	MS, RI
70	*n*-Octacosane	$C_{28}H_{58}$	48.412	0.54	2804	2800	Acyclic alkanes	MS, RI
71	Squalene	$C_{30}H_{50}$	48.949	0.31	2846	2847	Triterpenes	MS, RI
72	*n*-Nonacosane	$C_{29}H_{60}$	49.825	0.3	2909	2900	Acyclic alkanes	MS, RI
73	24-Norursa-3,12-diene	$C_{29}H_{46}$	52.355	0.31	3098	3105	Triterpenes	MS, RI
74	*n*-Hentriacontane	$C_{31}H_{64}$	52.52	0.2	3110	3100	Acyclic alkanes	MS, RI
75	Campesterol	$C_{28}H_{48}O$	54.895	0.65	3178	3131	Sterol	MS
76	**Stigmasterol**	$C_{29}H_{48}O$	55.410	**1.73**	3277	3275	Sterol	MS, RI
77	**γ-Sitosterol**	$C_{29}H_{50}O$	56.430	**3.54**	3343	3341	Sterol	MS, RI
78	Lupenone	$C_{30}H_{48}O$	57.605	0.43	3419	3384	Triterpenes	MS
79	4,22-Stigmastadiene-3-one	$C_{29}H_{46}O$	57.830	0.26	3430	3399	Sterol	MS
80	Lupeol	$C_{30}H_{50}O$	58.055	0.62	3441	3451	Triterpenes	MS, RI
81	4-Stigmasten-3-one (Sitostenone)	$C_{29}H_{48}O$	59.045	0.56	3445	3435	Sterol	MS, RI

Total hydrocarbons (%)	72.04
Total terpenes (%)	6.97
Total sterols (%)	6.74
Miscellaneous (%)	0.25
Total identified compounds (%)	86

RI: Retention index calculated on RTX-5MS column relative to *n*-alkane series (C_8–C_{40}), Compounds are listed in order of their elution on RTX-5MS GC column. MS: Identification based on mass spectral data and RI: identification based on comparison with published retention indices in National Institute of Standards and Technology NIST chemistry webbook library and identification of essential oil components by Gas Chromatography/Quadrupole Mass Spectrometry and literature.

Table S2: Minimal inhibitory concentration (µg/mL) and 90% minimal inhibitory concentration (µg/mL) of *n*-hexane extract and 50% concentration of *n*-hexane extract in combination with 50% concentration of isoniazid.

Samples	**MIC (µg/mL)**	**MIC_{90} (µg/mL)**

VP *n*-Hexane extract	62.5	45.7
50% concentration VP *n*-hexane extract +50% concentration isoniazid	31.4	13.2
Isoniazid (positive control)	0.24	0.17

Table S3: Free binding energies (Kcal/mol) of the major identified compounds within the active site of *Mtb* C171Q receptor KasA inhibitor (4C6X) using Discovery Studio 4.5 software.

Compound Name	**Free Binding Energy (ΔG) (Kcal/mol)**
n-Nonane	-33.34
n-Undecane	-32.51
2-Methyldecane	-31.96
6-Methylundecane	-31.91
n-Tetradecane	-31.78
n-Decane	-31.53
2,6-Dimethyloctane	-31.37
n-Pentadecane	-31.13
3-Methyl decane	-29.79
n-Dodecane	-29.39
2-Methyl undecane	-29.06
3,6-Dimethyl undecane	-27.16
2,3-Dimethy lnonane	-26.35
Butyl cyclohexane	-26.12
Pentyl cyclohexane	-24.91
Isoniazid	-20.85
(*E*)-*p*-Menthane	-19.07
Co-crystallized ligand (Thiolactomycin)	-10.59
(*E*)-Decahydronaphthalene	-10.35
2,3-Dimethyl-2-octene	0.64
γ-Sitosterol	FD
Stigmasterol	FD

FD failed to dock

Positive values indicate unfavorable binding

Figures (S1-S6)

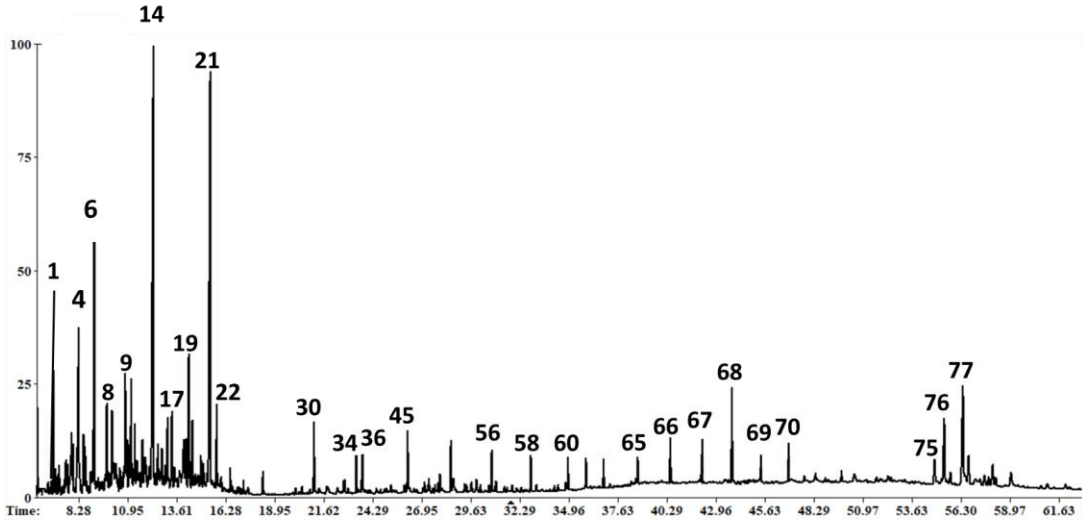

Figure S1. GC-MS chromatogram of the *n*-hexane extract of *Vitex pinnata* bark.

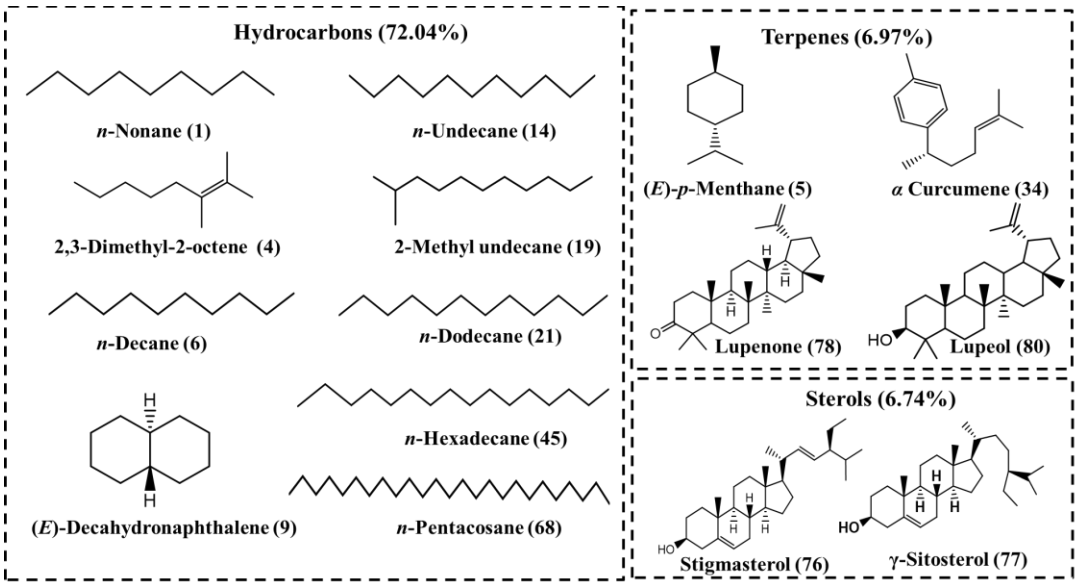

Figure S2. Major constituents of *n*-hexane extract *Vitex pinnata* bark identified using GC-MS.

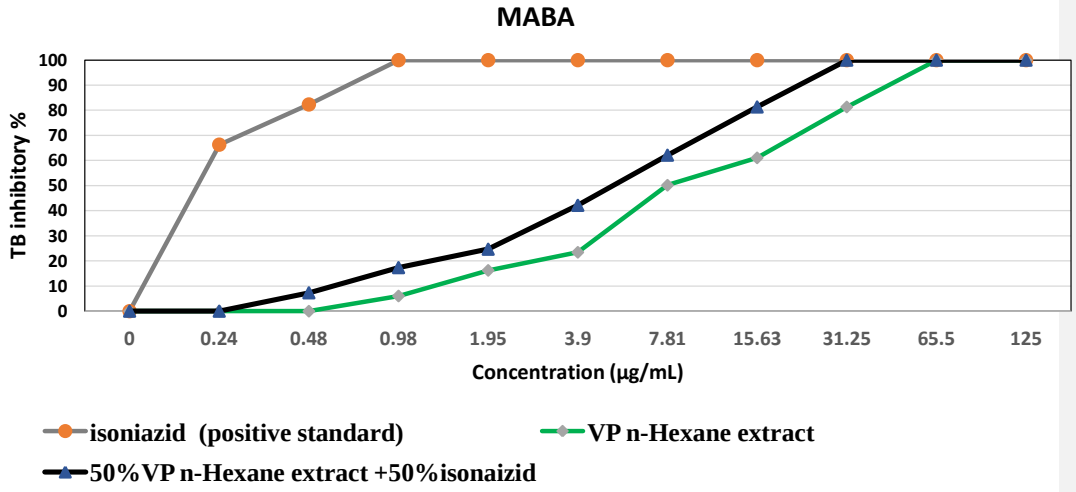

Figure S3. Effect of different concentration (µg/mL) of *n*-hexane extract and 50% concentration of *n*-hexane extract in combination with 50% concentration of isoniazid on TB inhibitory (%) in comparison with positive standard (isoniazid).

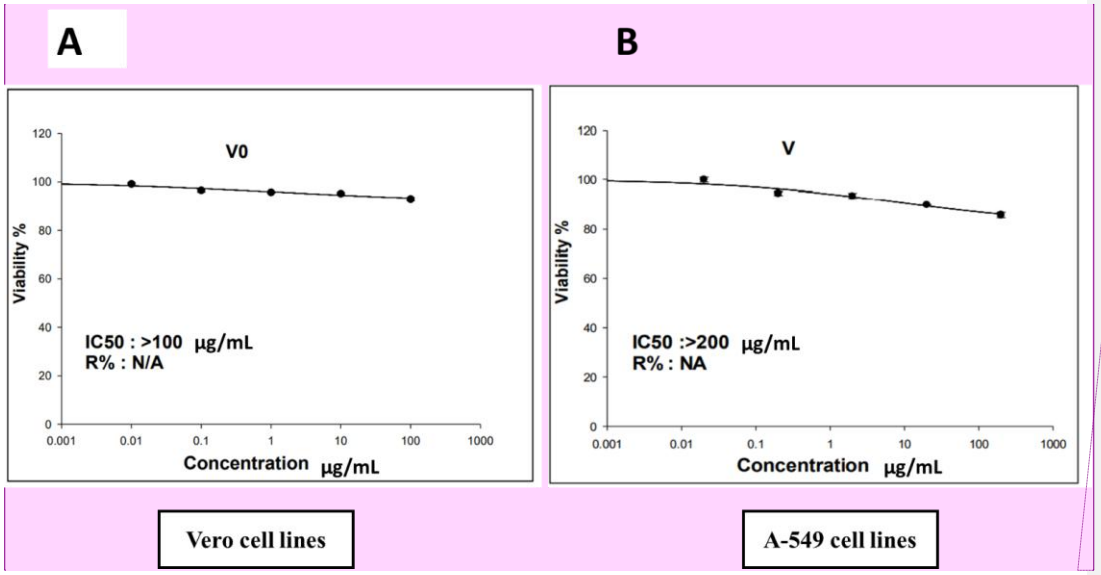

Comment [sa2]: µg/ml changed to µg/mL

Figure S4. Cytotoxic activity of *n*-hexane extract of *Vitex pinnata* bark on (**A**) Vero cell line, (**B**) A-549 cell line.

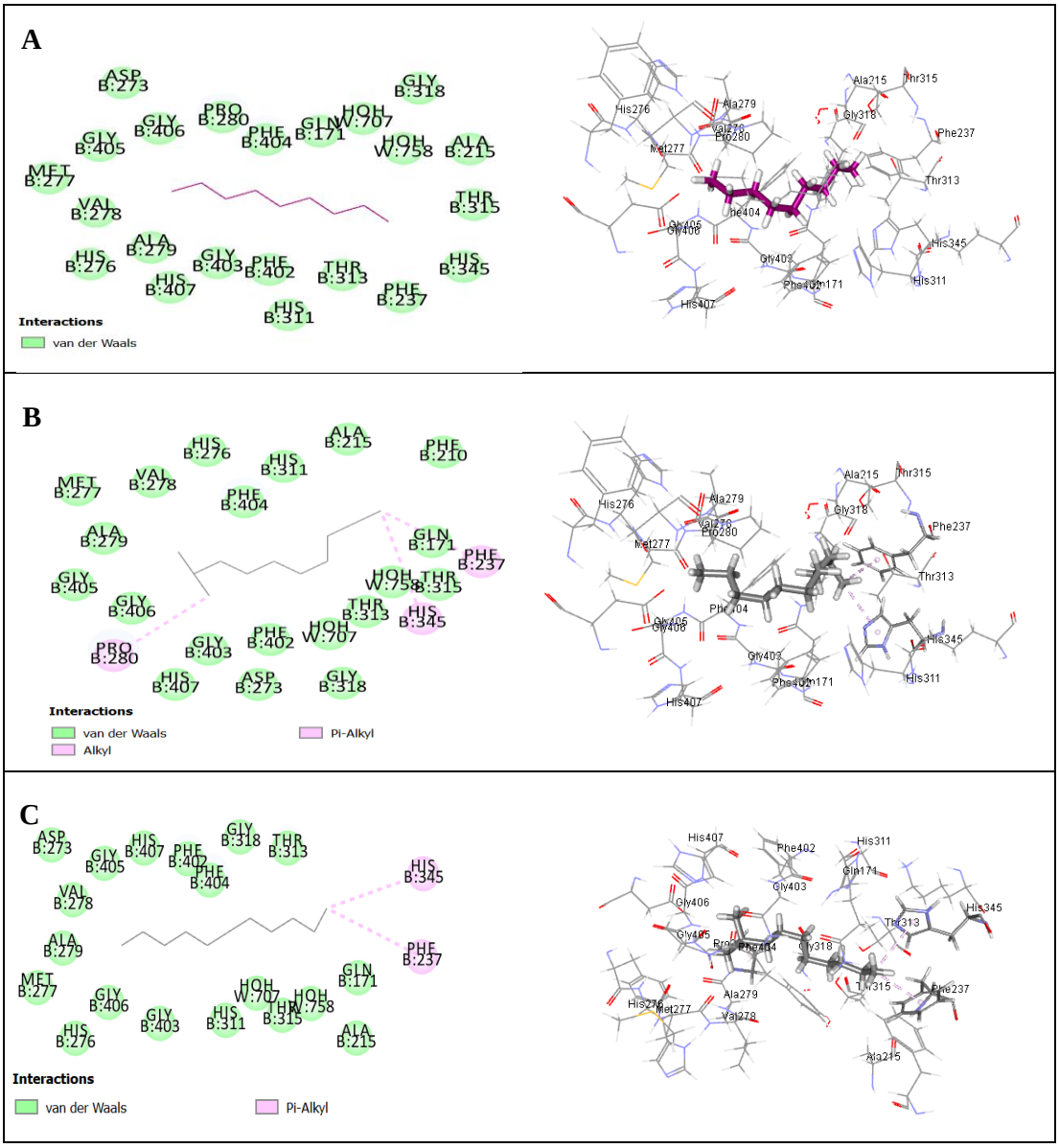
A
ASP B:273
GLY B:318
PRO B:280
HOH W:707
GLY B:406
GLY B:405
PHE B:404
GLN B:171
HOH W:758
ALA B:215
MET B:277
THR B:315
VAL B:278
ALA B:279
HIS B:276
GLY B:403
PHE B:402
THR B:313
HIS B:345
HIS B:407
PHE B:237
HIS B:311
Interactions
van der Waals
Ala215
Thr315
His276
Ala279
Gly318
Val278
Pro280
Phe237
Met277
Thr313
Ile404
Gly405
Gly406
His345
Gly403
Phe402
Gln171
His311
His407
B
HIS B:276
ALA B:215
PHE B:210
HIS B:311
MET B:277
VAL B:278
PHE B:404
ALA B:279
GLN B:171
PHE B:237
GLY B:405
HOH W:758
THR B:315
GLY B:406
THR B:313
HIS B:345
PHE B:402
HOH W:707
PRO B:280
GLY B:403
HIS B:407
ASP B:273
GLY B:318
Interactions
van der Waals
Pi-Alkyl
Alkyl
Ala215
Thr315
His276
Ala279
Gly318
Val278
Pro280
Phe237
Met277
Thr313
Ile404
Gly405
Gly406
His345
Gly403
Phe402
Gln171
His311
His407
C
ASP B:273
GLY B:318
THR B:313
HIS B:407
PHE B:402
GLY B:405
PHE B:404
HIS B:345
VAL B:278
ALA B:279
PHE B:237
MET B:277
GLN B:171
HOH W:707
HOH W:758
GLY B:406
THR B:315
GLY B:403
HIS B:311
HIS B:276
ALA B:215
Interactions
van der Waals
Pi-Alkyl
His407
Phe402
His311
Gln171
Gly403
Gly406
His345
Thr313
Gly405
Pro
Phe404
Gly318
Thr315
Phe237
Ala279
His276
Met277
Val278
Ala215

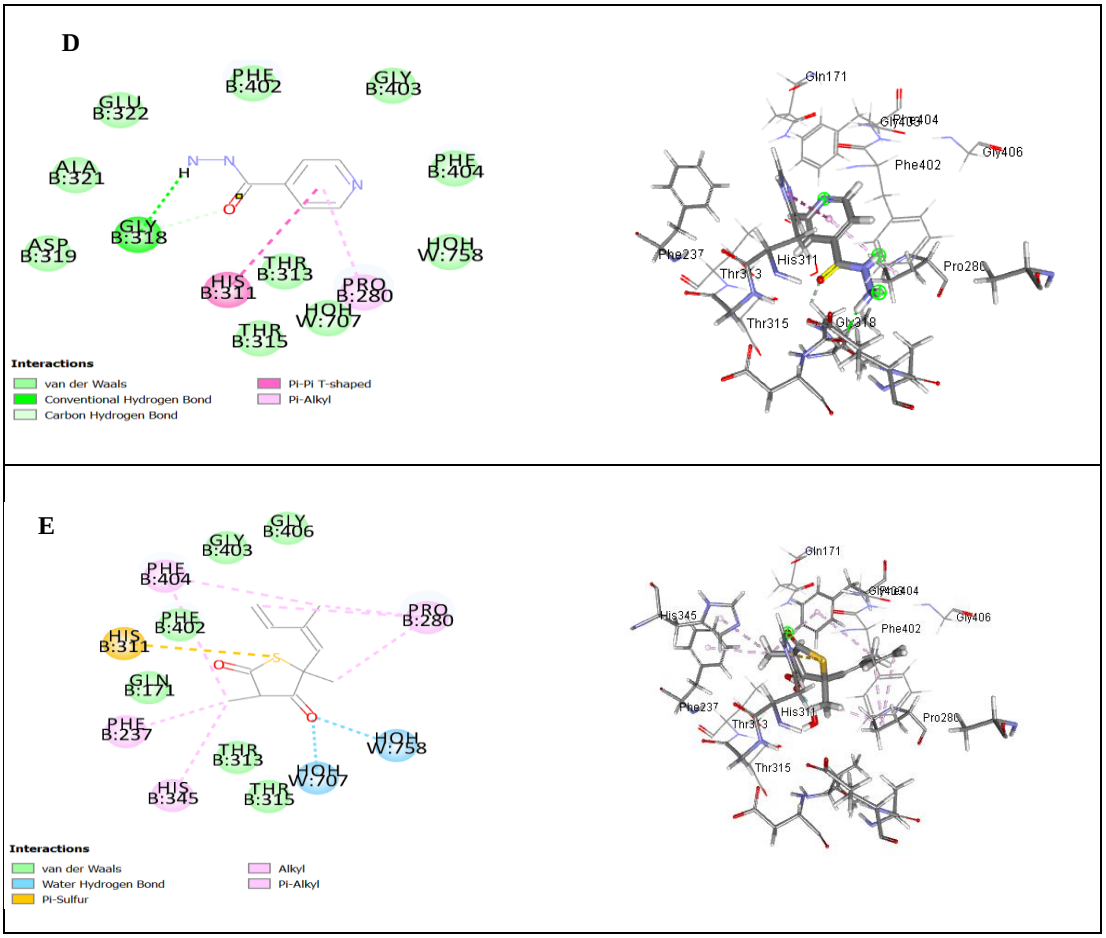

Figure S5. 2D and 3D binding behavior of *n*-nonane **(A)**, *n*-undecane **(B)**, 2-methyldecane **(C)**, isoniazid **(D)**, thiolactomycin; the co-crystallized ligand **(E)**, within the active site of *Mtb* C171Q receptor KasA inhibitor (4C6X) using C-docker protocol.

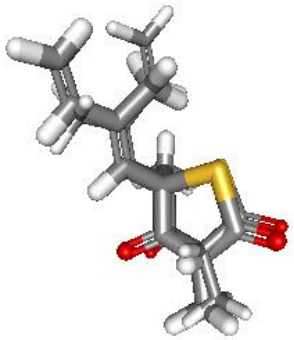

Figure S6. Validation of the docking experiment.

References

Abd El-Ghffar EA, El-Nashar HA, Eldahshan OA, Singab ANB. 2017. GC-MS analysis and hepatoprotective activity of the *n*-hexane extract of *Acrocarpus fraxinifolius* leaves against paracetamol-induced hepatotoxicity in male albino rats. Pharmaceutical biology. 55(1):441-449.

Abd El-Ghffar EA, Eldahshan OA, Barakat A, Efferth T. 2018. The prophylactic effect of a *Eugenia aquea* extract against oxidative stress and inflammation associated with the development of arthritis in an adjuvant-induced arthritis rat model. Food function. 9(12):6643-6651.

Abdel-Aziz MM, Elella MHA, Mohamed RR. 2020. Green synthesis of quaternized chitosan/silver nanocomposites for targeting *Mycobacterium tuberculosis* and lung carcinoma cells (A-549). International journal of biological macromolecules. 142:244-253.

Adams RP. 2007. Identification of essential oil components by gas chromatography/mass spectrometry: Allured publishing corporation Carol Stream, IL.

Ahmad B, Azam S, Bashir S, Khan I, Adhikari A, Choudhary MI. 2010. Anti-inflammatory and enzyme inhibitory activities of a crude extract and a pterocarpan isolated from the aerial parts of *Vitex agnus-castus*. Biotechnology Journal. 5(11):1207-1215.

Al-Sayed E, Gad HA, El-Kersh DM. 2021. Characterization of Four *Piper* Essential Oils (GC/MS and ATR-IR) Coupled to Chemometrics and Their anti-*Helicobacter pylori* Activity. ACS omega. 6(39):25652-25663.

Ashmawy AM, Ayoub IM, Eldahshan OA. 2021. Chemical composition, cytotoxicity and molecular profiling of *Cordia africana* Lam. on human breast cancer cell line. Natural Product Research. 35(21):4133-4138.

Ayoub IM, Korinek M, El-Shazly M, Wetterauer B, El-Beshbishy HA, Hwang T-L, Chen B-H, Chang F-R, Wink M, Singab ANB, et al. 2021. Anti-Allergic, Anti-Inflammatory, and Anti-Hyperglycemic Activity of *Chasmanthe aethiopica* Leaf Extract and Its Profiling Using LC/MS and GLC/MS. Plants. 10(6):1118.

Franzblau SG, Witzig RS, McLaughlin JC, Torres P, Madico G, Hernandez A, Degnan MT, Cook MB, Quenzer VK, Ferguson RM. 1998. Rapid, low-technology MIC determination with clinical *Mycobacterium tuberculosis* isolates by using the microplate Alamar Blue assay. Journal of clinical microbiology. 36(2):362-366.

Gad H, Al-Sayed E, Ayoub I. 2021. Phytochemical discrimination of *Pinus* species based on GC–MS and ATR-IR analyses and their impact on *Helicobacter pylori*. Phytochemical Analysis. 32(5):820-835.

Gamal El-Din MI, Youssef FS, Ashour ML, Eldahshan OA, Singab ANB. 2018. Comparative analysis of volatile constituents of *Pachira aquatica* Aubl. and *Pachira glabra* Pasq., their anti-Mycobacterial and anti-

Helicobacter pylori activities and their metabolic discrimination using chemometrics. Journal of Essential Oil Bearing Plants. 21(6):1550-1567.
Kamiloglu S, Sari G, Ozdal T, Capanoglu E. 2020. Guidelines for cell viability assays. Food Frontiers. 1(3):332-349.
Korany DA, Ayoub IM, Labib RM, El-Ahmady SH, Singab ANB. 2021. The impact of seasonal variation on the volatile profile of leaves and stems of *Brownea grandiceps* (Jacq.) with evaluation of their anti-mycobacterial and anti-inflammatory activities. South African Journal of Botany. 142:88-95.
Lawal T, Adeniyi B, Wan B, Franzblau S, Mahady G. 2011. *In-vitro* susceptibility of *Mycobacterium tuberculosis* to extracts of *Uvaria afzelli* Scott Elliot and *Tetracera alnifolia* Willd. African Journal of Biomedical Research. 14(1):17-21.
M Elkady W, Ayoub IM, Abdel-Mottaleb Y, ElShafie MF, Wink M. 2020. Euryops pectinatus L. Flower extract inhibits p-glycoprotein and reverses multi-drug resistance in cancer cells: A mechanistic study. Molecules. 25(3):647.
Nkenfou CN, Mawabo IK, Notedji A, Nkenfou J, Fokou PVT, Jouda JB, Kuiate J-R. 2015. *In vitro* antimycobacterial activity of six Cameroonian medicinal plants using microplate alamarBlue assay. International journal of mycobacteriology. 4(4):306-311.
Thabet AA, Ayoub IM, Youssef FS, Al Sayed E, Singab ANB. 2021. Essential oils from the leaves and flowers of *Leucophyllum frutescens* (Scrophulariaceae): phytochemical analysis and inhibitory effects against elastase and collagenase *in vitro*. Natural Product Research.1-5.